ACS APPLIED MATERIALS & INTERFACES

Research Article

www.acsami.org

Cross-links in Carbon Nanotube Assembly Introduced by Using Polyacrylonitrile as Precursor

Yanbin Cui and Mei Zhang*

Department of Industrial and Manufacturing Engineering, FAMU-FSU College of Engineering, High-Performance Materials Institute, Florida State University, 2525 Pottsdamer Street, Tallahassee, Florida 32310, United States

Supporting Information

ABSTRACT: Individual carbon nanotube (CNT) exhibits extraordinary mechanics. However, the properties of the macroscopic CNT-based structure, such as CNT fibers and films, are far lower than that of individual CNT. One of the main reasons is the weak interaction between tubes and bundles in the CNT assemblies. It is understood that the cross-links in CNT assembly play a key role to improve the performance of CNT-based structure. Different approaches have been taken to create CNT joints. Most of these approaches focus on connecting CNTs by generating new covalent bonding between tubes. In this work, we intend to reinforce the CNT network by locking the contacted CNTs. Polyacrylonitrile (PAN) was used as precursor because PAN can form graphitic structures after carbonization. The freestanding superthin CNT sheet and CNT yarn were used to evaluate the effects of the PAN precursor to form cross-links between CNTs. The tensile strength of CNT yarn is improved when the yarn is partially infiltrated with PAN and consequently carbonated. High-resolution transmission electron microscopy observation of the sheets shows that graphite structures are formed and cross-link CNTs in CNT assembly.

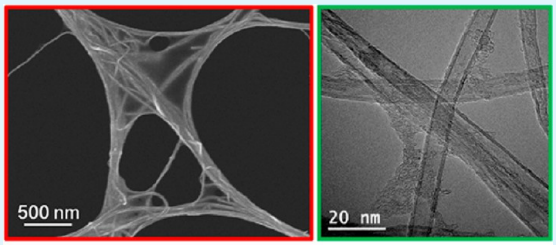

Cross-linked CNTs

KEYWORDS: *carbon nanotube, cross-link, polyacrylonitrile, carbon nanotube sheet, carbon nanotube yarn*

1. INTRODUCTION

Because of their extremely mechanical properties, as well as their superior electrical and thermal conductivities,[1] carbon nanotubes (CNTs) have attracted tremendous research interest in the past two decades.[2] Numerous applications have been proposed for CNT use in different fields.[3−11] It is a key step to realize their extensive application through assembly on a macroscopic scale with controlled orientation and configuration.[12] In recent years, much attention has been devoted to the macroscopic assembly of CNTs. Consequently, a range of macroscopic CNT-based structures have been fabricated, including forests,[13] fibers,[14] films,[15] sheets,[16] and foams.[17] However, these CNT-based structures have not fully produced the mechanical characteristics of their nanotube building blocks.[18] Because of weak intertube interactions, the actual mechanical properties of these CNT-based structures are still several orders of magnitude lower than that of an individual CNT.

The supporting forces for macroscopic assembly of CNTs are van der Waals force, entanglement of CNTs, or intercalation by anionic ions.[19] The CNT-based structures will undergo structural collapse or plastic deformation with a reduction in compressive strength when they are subjected to cyclic strain.[20] Meanwhile, large deformations will be observed at the struts and junctions of the intertube structure of CNT-based assemblies. For improving the mechanical properties of CNT-based structures, cross-links are in fact needed for load transfer between different CNTs.[21] Meanwhile, the cross-links can also improve electron and thermal transport among CNTs.

Introducing stable cross-links between CNTs, without significantly degrading their unique properties in the process, would bring their application closer to reality.[22] In order to utilize the characteristic properties of a single CNT on a macroscopic scale, a few approaches for cross-linking CNT joints have been reported, including irradiation, electron or iron beam deposition,[23] soldering,[24] chemical modifying[25] and doping.[26] For example, Peng et al. cross-linked CNTs using electron beam deposition inside a transmission electron microscope, which caused the CNTs to connect by accumulating amorphous carbon at the CNT junctions.[23] However, the well-ordered structure of CNTs will transform into amorphous carbon around the junctions and the properties of CNT will be degraded at high dose irradiation. Using Co as soldering material, Wang et al. joined different CNTs at crossing points by electron irradiation at high temperatures in an electron microscope.[24] By applying an amidation-type grafting reaction with amino-functionalized alternating polyketones, Picchioni et al. functionalized CNTs and created interconnection between CNTs using polyamines as cross-linking agents.[25] Ajayan et al. synthesized bulk three-dimentional macroscale CNT solids and established covalent

Received: June 11, 2013
Accepted: July 31, 2013
Published: July 31, 2013

   dx.doi.org/10.1021/am4022686 | ACS Appl. Mater. Interfaces 2013, 5, 8173−8178

junctions between CNTs via a boron-doping strategy during chemical deposition (CVD).[26] However, the additives can bring impurities and defects into the CNTs which are detrimental to the performance of CNT-based assemblies.[27] It is still a major challenge to develop a simple and scalable method to cross-link different CNTs in bulk CNT structures without compromising their key characteristic properties.

Generally, polymers can be utilized to reinforce the structural integrity of the CNT network.[28] Polyacrylonitrile (PAN) is the predominant precursor for manufacturing high performance carbon fibers and a very promising precursor for nanostructured carbons, such as highly oriented graphite nanosheets.[29] PAN can be carbonized to form strong C−C bonding when it is treated in an inert gas over 1000 °C. Furthermore, PAN has interacts favorably with CNTs.[30] Most recently, Islam et al. fabricated graphene-coated CNT aerogels by coating prefoamed CNT aerogels with a PAN polymer.[20] The PAN enhancement does not affect the structural integrity of the CNT foam or the porosity of the nanotube network. But the heating process and morphological change of PAN were not explored in detail. In this work, we used PAN as a precursor to form all-carbon cross-links between CNTs and investigated the morphological change of PAN and its reinforcement in CNT assembly. Because there are many joints between individual CNTs, individual CNT and CNT bundle, as well as CNT bundles, freestanding superthin CNT sheets are used to explore the strengthening of CNT assemblies through heat treatment with PAN. Because CNT's network is clear in the sheet and the sheets are free-standing, we can directly observe the joints in the sheet and create joints by stacking sheets together in desired alignment directions. We observed that PAN was concentrated at the CNT joints and changed into graphitic structures after carbonization treatment, which enhanced the intertubular connections within the CNT assembly.

2. EXPERIMENTAL SECTION

2.1. Synthesis of Multiwalled CNT Array. The synthesis of multiwalled CNT array is reported in detail elsewhere.[13] Briefly, a Si wafer with a 600 nm SiO_2 layer was used as a substrate. A catalyst film of Fe (0.5 nm) was deposited on the Si wafer by electron-beam evaporation (Edwards EB3 Electron Beam Evaporator). The CNT arrays were then synthesized in a three-zone quartz tube furnace (Easy-Tube 3000, First-Nano). The reaction chamber was a quartz tube with 5-in. diameter. The substrates were placed in the middle of the quartz tube, which was pumped down to 0.1 Torr to remove the ambient gas. The total pressure was maintained at 1 atm throughout. The furnace was heated up to growth temperature (690−780 °C) at 20 °C/min and under 5.0 SLPM Ar flow. Then, C_2H_2 (99.6%) and/or H_2 (99.9999%) were introduced into the reactor and the CNT arrays were synthesized at the growth temperature for a certain time. Finally, the acetylene and hydrogen gas flows were turned off and the furnace was cooled to room temperature under continuous Ar gas flow.

2.2. Fabrication of PAN-Coated CNT Sheets. CNT sheets were made by drawing CNTs directly from a sidewall of the prepared CNT array.[13] The PAN powder (M.W. 150,000 g/mol) was dissolved in dimethyl formamide (DMF) to form a homogeneous solution. Two CNT sheets were cross-stacked with the direction of CNTs of a latter layer perpendicular to that of a former one. The concentrations of PAN/DMF for CNT sheets were 0.01, 0.05, 0.1, and 0.2 wt %, respectively. CNT yarns were used to evaluate the strength of CNT assemblies through heat treatment with PAN. CNT yarn was spun from the CNT array.[14] The concentrations of PAN/DMF for the yarns were 1, 3, and 5 wt %, respectively. The CNT sheets or yarns were dipped perpendicularly into the PAN/DMF solution and immersed in the solution for 5 min, then pulled out perpendicularly. For comparison, CNT sheets and yarns were also dipped and densified in isopropanol (IPA). The PAN-coated and IPA-densified CNT sheets or yarns were dried in a vacuum oven at 70 °C for 12 h to ensure complete removal of DMF. Finally, the PAN polymer was pyrolyzed via a two-step process.[26] In the first step (stabilization), the samples were heated in a tube furnace (Eurotherm Carbolite) from room temperature to 280 °C at 2 °C/min, followed by an isothermal hold for 3h in air. The samples were then cooled to room temperature. In the second step (carbonization), the stabilized samples were pyrolyzed at 1000 °C in nitrogen gas (80 mL/min) at 1 atm for 1 h.

2.3. Characterization. Scanning electron microscopy (SEM, JEOL-JSM7401F, 10 KV) was used to characterize the morphology of PAN-coated CNT sheets. High-resolution transmission electron microscopy (HRTEM, JEM-ARM200F, 200 KV) was used to observe the structures around CNT joints. Mechanical analysis of the yarns was performed on a DMA Q800 machine (TA Instruments, Inc.), which has a 18 N maximum load cell and an accuracy of 0.1 mN. The rate of stretching and the initial gap between grips were 0.01 mm/s and 5 mm, respectively. The diameter of CNT yarns were measured by SEM and used to determine the cross-section area of CNT yarn for calculating tensile strength.

3. RESULTS AND DISCUSSION

For investigation the formation of cross-links between CNT through heat treatment with PAN, the cross-stacked CNT sheets were dipped into PAN/DMF solutions and the microstructure of PAN-coated CNT sheets were observed using SEM and HRTEM. For comparison, a cross-stacked sheet was dipped in isopropanol (IPA). The CNT sheets were densified in thickness during drying and some shrinkage in plane. Figure 1 shows SEM images of the IPA densified CNT sheets and PAN-infiltrated CNT sheets, which were dried in air and further dried at 70 °C for 12 h in a vacuum oven. The morphology of the IPA densified sheet is shown in panels a and b in Figure 1. There are many joints between individual CNTs,

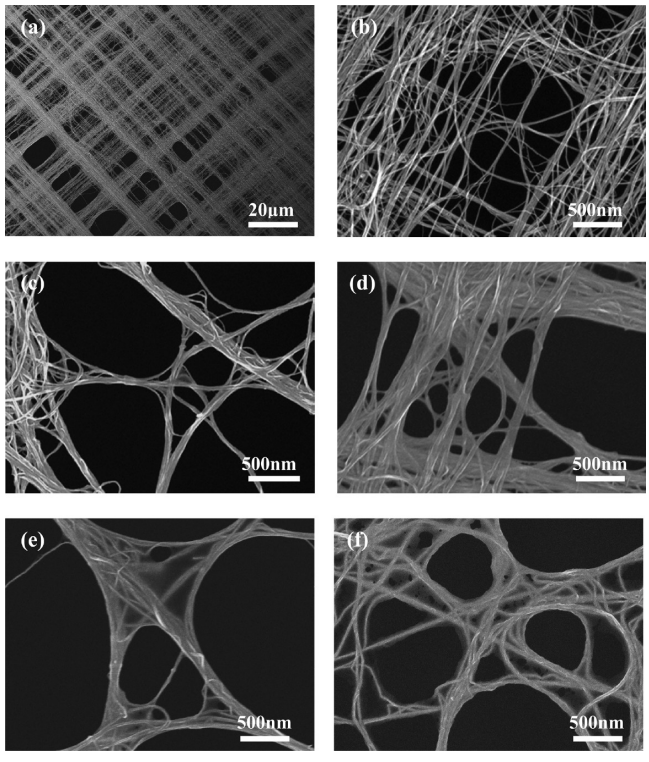

Figure 1. SEM images of (a, b) CNT sheets and CNT sheets dipped into PAN/DMF solution with concentration of (c) 0.01, (d) 0.05, (e) 0.1, and (f) 0.2 wt %.

individual CNT and CNT bundle, as well as CNT bundles in the cross-stacked CNT sheets. The surface of the CNT was clean and there are no catalyst particles on CNT sheets. Therefore, CNT sheets are suitable for investigating the morphology of PAN-coated CNT during the heating process. As shown in Figure 1c-1f, PAN molecules were brought to the CNT junctions by capillary force due to the evaporation of DMF and concentrated there.[17] When the concentration of PAN/DMF was 0.01 wt %, there was a small amount of PAN on CNT joints and some CNT joints were not covered by PAN (Figure 1c). With increased concentration of PAN/DMF (up to 0.05 wt %), PAN was concentrated at all CNT joints, and the CNTs were better connected by PAN (Figure 1d). When the concentration of PAN/DMF was increased up to 0.1 wt %, the amount of PAN at CNT joints increased and a PAN film was formed around CNT junctions (Figure 1e). At the highest concentration of PAN/DMF (0.2 wt %), a large amount of PAN was accumulated on CNT joints and CNT surfaces were coated by a layer of PAN (Figure 1f and Figure S1 in the Supporting Information).

During the stabilization step, the sample was stabilized at 280 °C in air. This process is intended to avoid excessive volatization of elemental carbon in the subsequent carbonization step.[31] The stretched chain molecule PAN is transformed into a nonmeltable conjugated structure by cyclization, dehydrogenation, and oxidation.[32] Meanwhile, there was a dimensional shrinkage of the PAN polymer on a macroscopic scale.[33] Figure 2 shows SEM images of PAN-coated CNT sheets after stabilization at 280 °C. As shown in Figure 2, PAN-coated CNT sheets present a change in morphology in comparison to Figure 1 and PAN around CNT joints shrank to the CNT joints after stabilization. When the concentration of PAN/DMF was lower than 0.05 wt %, PAN at the CNT joints was not visible at the same magnification as Figure 1 because of the shrinking of PAN. The film of PAN was broken and PAN shrank at CNT joints after stabilization when the concentration of PAN/DMF was higher than 0.1 wt % (Figure 2c, d). Some CNT surfaces were still covered by stabilized PAN after stabilization because of the high concentration of PAN/DMF.

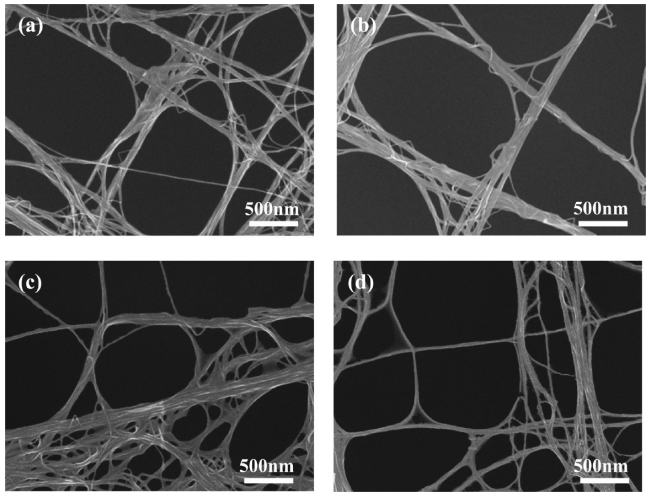

Figure 2. PAN-infiltrated CNT sheets after 280 °C treatment. (a–d) PAN/DMF solution with the concentration of (a) 0.01, (b) 0.05, (c) 0.1, and (d) 0.2 wt %, respectively.

In the carbonization step, PAN-infiltrated CNT sheets were heated to 1000 °C in a nitrogen environment. In this step, oxygen and the heterocyclic nitrogen were split off, and the PAN-derived conjugated structure was converted into graphitic structures by dehydrogenation and denitrogenation.[32,33] The conversion of stabilized PAN to graphitic structures that was accompanied by a significant volume decrease (by a factor of 2–3) if the graphitic structures formed from PAN did not have internal microporous voids.[29] Figure 3 shows the SEM images of PAN-infiltrated CNT sheets after carbonization. As shown in Figure 3, no significant structural changes were observed for the CNT sheets, which indicate that our CNT sheets are thermally stable up to 1000 °C. Because PAN was further shrunk in the carbonization process, PAN at the CNT joints are not visible at the same magnification as in Figure 2. The detailed microstructure of the graphitic structures formed from PAN at the joints between CNTs was investigated using HRTEM.

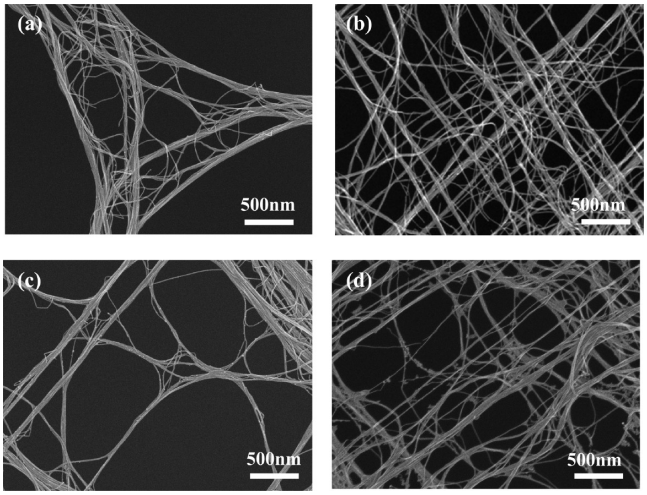

Figure 3. PAN-infiltrated CNT sheets after 1000 °C treatment. (a–d) PAN/DMF solution with the concentration of (a) 0.01, (b) 0.05, (c) 0.1, and (d) 0.2 wt %, respectively.

Figure 4 are the HRTEM images of a PAN-infiltrated CNT sheet after carbonization at 1000 °C. The concentration of the PAN/DMF solution was 0.1 wt %. Though PAN was not observed in the SEM images (Figure 3), it can be seen that cross-links have been formed around the joints of CNTs in their HRTEM images (Figure 4a, b). Typically, PAN-based fibers are carbonized in the range of 2500–3000 °C in order to develop graphitic structure.[34] The presence of CNTs can promote the graphitization of PAN at a relatively low temperature.[35] As shown in Figure 4b, PAN was converted into well-ordered graphitic structures after carbonization and the tubes are cross-linked by graphitic structures agglomerating nearby the crossing position of different CNTs. Partial CNT surfaces were also coated with a graphite layer (Figure 4c). Meanwhile, some discrete multilayers of graphene were formed on the surface of CNTs (arrows in Figure 4d). Generally, there are defects on the wall of CNT prepared by CVD methods. The defects on CNT walls could be the sites for the carbonized PAN to covalently graft on to the CNTs' surface. On the other hand, the carbonized PAN can also noncovalently attach to CNT surface by $\pi-\pi$ stacking. In our system, the position of the carbonized PAN on CNTs plays an important role in the improvement of the mechanical properties. When the graphite layer bridges different CNTs and accumulates at the joints of

dx.doi.org/10.1021/am4022686 | ACS Appl. Mater. Interfaces 2013, 5, 8173–8178

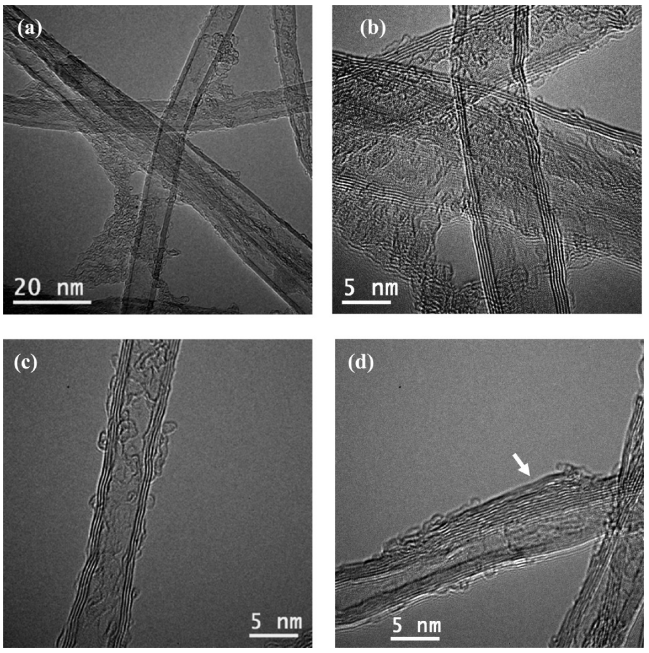

Figure 4. HRTEM images of CNT sheet infiltrated with PAN/DMF (0.1 wt %) after carbonization at 1000 °C.

CNTs as shown in Figures 4a and 4b, it contributes to the strength increase by improving the load transfer between different CNTs, especially when there is covalent bonding at the interface. The graphitic structures at the CNT joints can confine CNT sliding because the graphitic structures can "lock" CNTs like a "jacket". Because the nanotubes in the sheet are long and several joints may form along a single nanotube, the "locking" and sliding will definitely increase the robustness of the CNT networks. However, if the graphite layer attached only on CNT surface, its contribution to the improvement of mechanical properties would be limited. This is demonstrated by the experiment of changing the concentration of PAN in DMF applied to CNT yarns.

CNT yarns were used to evaluate the strengthening of CNT assemblies through heat treatment with PAN. Because CNTs in yarn are densely packed, the infiltration of the PAN is limited to the surface. Figure S2 in the Supporting Information shows that the infiltration depth is around 2 μm in a CNT yarn with 25 μm diameter. The mechanical properties of CNT yarn and PAN-coated CNT yarn after carbonization are shown in Figure 5. Figure 5a shows the typical stress–strain curves of the samples with and without PAN infiltration and after 1000 °C thermal treatment. From stress–strain curves of the samples, we obtain the strength, Young's modulus, and toughness of the yarns. These parameters are shown as a function of the concentration of PAN/DMF in Figure 5b–d. As indicated in panels a and b in Figure 5, the measured tensile strength of pristine CNT yarn was 367 ± 10 MPa. It should be noted that these values were engineer stress based on cross-sectional areas measured by SEM for the unstressed yarn.[14] Besides, the measured tensile strength of CNT yarn heat-treated at 1000 °C is consistent with the tensile strength of CNT yarn that has not been heated up to 1000 °C,[14] which means that the heat treatment process did not reduce the strength of CNT yarn. The observed stress increased to 480 ± 24 MPa (i.e., 30% increasing) for PAN (with the concentration of 1 wt %)-infiltrated CNT yarns after carbonization. With increasing of the concentration of PAN/DMF, the stress of PAN-coated CNT yarns are almost constant, which fall in the range of 470–480 MPa.

The improved stress suggests that the load transfer was improved by nanotube cross-linking.[36,37] It should be noted

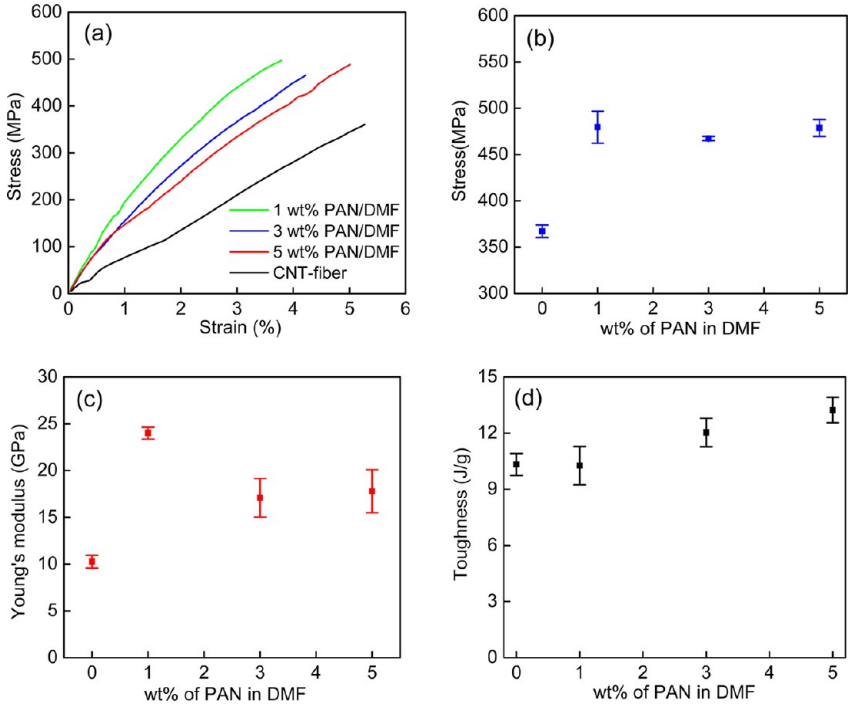

Figure 5. Mechanical properties of CNT yarn and PAN-coated CNT yarn after carbonization. (a) Representative stress–strain curves for the yarn used in this work. (b) Tensile strength, (c) Young's modulus, and (d) toughness as a function of concentration of PAN/DMF. The errors represent standard errors calculated from 4 measurements.

that the tensile strength of our PAN-coated CNT yarns was lower than that of the CNT yarns reported in the literature.[38] Several factors lead to the lower tensile strength of our CNT yarns. One is that we did not heavily densify the yarns through twisting in order to have higher PAN infiltration. The strength of the yarn strongly depends on the twist level because twist spun is a densification process. Higher-level densification leads to higher mechanical strength because it increases the contacts between CNTs and, therefore, the load transfer. The others are that the yarns are porous and the infiltration of PAN is limited to around 2 μm under the yarn's surface. Position of the graphitic structures form on CNTs is another important factor. As indicated in Figure 4, CNTs could be cross-linked by graphitic structures when the concentration of PAN/DMF is 0.1 wt %. When the PAN concentration was increased from 1 to 5 wt %, more graphitic structures (including carbon vesicles) with CNTs exist in the samples. However, more carbonized PAN attached on CNT surface when the PAN concentration is higher than 1 wt %. As a result, the engineer strength of the yarns does not increase as the increase of the PAN concentration in this work.

Compared to the pristine CNT yarns, the elongation to break value of 1 wt % PAN-coated CNT yarn was decreased from 5.27% to 3.80%. When the weight percent of PAN in DMF solution increased from 1 to 5 wt %, the strain of PAN-coated CNT yarn increased to 5.01%, which is still slightly smaller than that of the pristine yarn. Because the slippage of CNTs is impeded by the cross-links between tubes,[39] the strain of PAN-coated CNT yarns was smaller than that of pristine one. The Young's modulus of the pristine CNT yarns and 1 wt % PAN-coated CNT yarns were 10.3 ± 1.0 GPa and 24.0 ± 0.9 GPa, respectively (Figure 5c). Because the strain of 1 wt % PAN-coated CNT yarns dropped from 5.27 to 3.80%, the toughness of 1 wt % PAN-coated CNT yarns was almost the same as that of pristine CNT yarns (Figure 5d). When the weight percent of PAN in DMF solution increased from 1 to 5 wt %, the toughness of PAN-coated CNT yarns increased approximately linearly from 10.3 ± 1.4 to13.2 ± 1.0 J/g. Because of the formation of cross-links between CNTs, the sliding of CNT is confined by the graphitic structure concentrated at the CNT joints. Therefore, greater stress would be required to cause a given amount of junction mention of PAN-coated CNT yarns. Thus, failure would tend to occur at higher stresses and lower strains for PAN-coated CNT yarns, which may result in an increased toughness.[39] A limited mechanical property improvement for CNT yarns in this work is also related with the PAN-coating process. Because of the short time dip-coating method, PAN merely infiltrates the core of the CNT yarn and only fills around 2 μm under the surface of the CNT yarns (see Figure S2 in the Supporting Information). It should be noted that there is plenty of room to improve the mechanical performance of PAN-coated CNT yarns by using other methods to penetrate PAN into CNT yarn completely.

4. CONCLUSIONS

In summary, PAN was used as a precursor to form all-carbon cross-links between CNTs. Freestanding superthin CNT sheets were used to explore the morphological change of PAN and CNT yarns and were used to evaluate the reinforcement of CNT assemblies through heat treatment with PAN. PAN polymer was infiltrated into CNT sheets and yarns by the dip-coating method and graphitized by a two-step process. SEM and HRTEM images indicate that PAN polymer converts into graphitic structures and accumulates on the joints of CNTs to form all-carbon cross-links between nanotubes after carbonization. Meanwhile, some CNT surfaces were covered by layers of graphitic structure. With limited infiltration with PAN and carbonization, the tensile strength and Young's modulus of CNT yarn increased from 367 ± 10 MPa and 10.3 ± 1.0 GPa to 480 ± 24 MPa and 24.0 ± 0.9 GPa, respectively, which demonstrate that the cross-links improve the load transfer between CNTs.

■ ASSOCIATED CONTENT

Supporting Information

SEM and TEM images of PAN-infiltrated CNT sheets and CNT yarns. This material is available free of charge via the Internet at http://pubs.acs.org/.

■ AUTHOR INFORMATION

Corresponding Author

*E-mail: mzhang@eng.fsu.edu (M.Z.).

Notes

The authors declare no competing financial interest.

■ ACKNOWLEDGMENTS

The TEM observation was carried out at the Florida State University (FSU) TEM facility, which is funded by the FSU Research Foundation and supported by the NHMFL with NSF DMR-0654118 and the State of Florida.

■ REFERENCES

(1) Chen, H.; Roy, A.; Baek, J. B.; Zhu, L.; Qu, J.; Dai, L. M. *Mater. Sci. Eng., R* **2010**, *70*, 63−91.
(2) Gogotsi, Y. *Science* **2010**, *330*, 1332−1333.
(3) Small, W. R.; Panhuis, M. I. H. *Small* **2007**, *3*, 1500−1503.
(4) Green, M. J.; Behabtu, N.; Pasquali, M.; Adams, W. W. *Polymer* **2009**, *50*, 4979−4997.
(5) Ding, M. N.; Star, A. *Angew. Chem., Int. Ed.* **2012**, *51*, 7637−7638.
(6) Fan, S. S.; Chapline, M. G.; Franklin, N. R.; Tombler, T. W.; Cassell, A. M.; Dai, H. J. *Science* **1999**, *283*, 512−514.
(7) Zhang, L. L.; Zhao, X. S. *Chem. Soc. Rev.* **2009**, *38*, 2520−2531.
(8) Cheng, F. Y.; Tao, Z. L.; Liang, J.; Chen, J. *Chem. Mater.* **2008**, *20*, 667−681.
(9) Cao, Q.; Rogers, J. A. *Adv. Mater.* **2009**, *21*, 29−53.
(10) Avouris, P.; Chen, Z. H.; Perebeinos, V. *Nat. Nanotechnol.* **2007**, *2*, 605−615.
(11) Wei, D. C.; Liu, Y. Q. *Adv. Mater.* **2008**, *20*, 2815−2841.
(12) Boncel, S.; Sundaram, R. M.; Windle, A. H.; Koziol, K. K. K. *ACS Nano* **2011**, *5*, 9339−9344.
(13) Yamada, T.; Namai, T.; Hata, K.; Futaba, D. N.; Mizuno, K.; Fan, J.; Yudasaka, M.; Yumura, M.; Iijima, S. *Nat. Nanotechnol.* **2006**, *1*, 131−136.
(14) Zhang, M.; Atkinson, K. R.; Baughman, R. H. *Science* **2004**, *306*, 1358−1361.
(15) Cao, A. Y.; Dickrell, P. L.; Sawyer, W. G.; Ghasemi-Nejhad, M. N.; Ajayan, P. M. *Science* **2005**, *310*, 1307−1310.
(16) Zhang, M.; Fang, S. L.; Zakhidow, A. A.; Lee, S. B.; Aliev, A. E.; Williams, C. D.; Atkinson, K. R.; Baughman, R. H. *Science* **2005**, *309*, 1215−1219.
(17) Chakrapani, N.; Wei, B. Q.; Carrillo, A.; Ajayan, P. M.; Kane, R. S. *Proc. Natl. Acad. Sci. U.S.A.* **2004**, *101*, 4009−4012.
(18) Shim, B. S.; Zhu, J.; Jan, E.; Critchley, K.; Ho, S.; Podsiadlo, P.; Sun, K.; Kotov, N. A. *ACS Nano* **2009**, *3*, 1711−1722.
(19) Cha, S. I.; Kim, K. T.; Lee, K. H.; Mo, C. B.; Jeong, Y. J.; Hong, S. H. *Carbon* **2008**, *46*, 482−488.

(20) Kim, K. H.; Oh, Y.; Islam, M. F. *Nat. Nanotechnol.* **2012**, *7*, 562−566.
(21) Pugno, N. M. *Mater. Today* **2010**, *13*, 40−43.
(22) Kis, A.; Csanyi, G.; Salvetat, J. P.; Lee, T. N.; Couteau, E.; Kulik, A. J.; Benoit, W.; Brugger, J.; Forro, L. *Nat. Mater.* **2004**, *3*, 153−157.
(23) Wang, M. S.; Wang, J. Y.; Chen, Q.; Peng, L. M. *Adv. Funct. Mater.* **2005**, *15*, 1825−1831.
(24) Rodriguez-Manzo, J. A.; Wang, M. S.; Banhart, F.; Bando, Y.; Golberg, D. *Adv. Mater.* **2009**, *21*, 4477−4482.
(25) Zhang, Y. C.; Broekhuis, A. A.; Stuart, M. C. A.; Landaluce, T. F.; Fausti, D.; Rudolf, P.; Picchioni, F. *Macromolecules* **2008**, *41*, 6141−6146.
(26) Hashim, D. P.; Narayanan, N. T.; Romo-Herrera, J. M.; Cullen, D. A.; Hahm, M. G.; Lezzi, P.; Suttle, J. R.; Kelkhoff, D.; Munoz-Sandoval, E.; Ganguli, S. *Sci. Rep.* **2012**, *2*, 363 DOI: 10.1038/srep00363.
(27) Fu, Y. F.; Carlberg, B.; Lindahl, N.; Lindvall, N.; Bielecki, J.; Matic, A.; Song, Y. X.; Hu, Z. L.; Lai, Z. H.; Ye, L. L. *Adv. Mater.* **2012**, *24*, 1576−1581.
(28) Skaltsas, T.; Avgouropoulos, G.; Tasis, D. *Microporous Mesoporous Mater.* **2011**, *143*, 451−457.
(29) Kruk, M.; Dufour, B.; Celer, E. B.; Kowalewski, T.; Jaroniec, M.; Matyjaszewski, K. *J. Phys. Chem. B* **2005**, *109*, 9216−9225.
(30) Chae, H. G.; Sreekumar, T. V.; Uchida, T.; Kumar, S. *Polymer* **2005**, *46*, 10925−10935.
(31) Chen, J. C.; Harrison, I. R. *Carbon* **2002**, *40*, 25−45.
(32) Fitzer, E.; Frohs, W.; Heine, M. *Carbon* **1986**, *24*, 387−395.
(33) Luo, X. F.; Mather, P. T. *Soft Matter* **2010**, *6*, 2146−2149.
(34) Chae, H. G.; Minus, M. L.; Rasheed, A.; Kumar, S. *Polymer* **2007**, *48*, 3781−3789.
(35) Chae, H. G.; Choi, Y. H.; Minus, M. L.; Kumar, S. *Compos. Sci. Technol.* **2009**, *69*, 406−413.
(36) Ogino, S. I.; Sato, Y.; Yamamoto, G.; Sasamori, K.; Kimura, H.; Hashida, T.; Motomiya, K.; Jeyadevan, B.; Tohji, K. *J. Phys. Chem. B* **2006**, *110*, 23159−23163.
(37) Chen, I. W. P.; Liang, R.; Zhao, H. B.; Wang, B.; Zhang, C. *Nanotechnology* **2011**, *22*, 485708.
(38) Liu, K.; Sun, Y. H.; Lin, X. Y.; Zhou, R. F.; Wang, J. P.; Fan, S. S.; Jiang, K. L. *ACS Nano* **2010**, *4*, 5827−5834.
(39) Khan, U.; O'Connor, I.; Gun'ko, Y. K.; Coleman, J. N. *Carbon* **2010**, *48*, 2825−2830.